Direct Evidence for *Sphingomonas* sp. A1 Periplasmic Proteins as Macromolecule-Binding Proteins Associated with the ABC Transporter: Molecular Insights into Alginate Transport in the Periplasm[†,‡]

Keiko Momma,[§] Yumiko Mishima,[§] Wataru Hashimoto,[§] Bunzo Mikami,[||,⊥] and Kousaku Murata*[,§,⊥]

Laboratory of Basic and Applied Molecular Biotechnology, Division of Food Science and Biotechnology, Graduate School of Agriculture, Kyoto University, Uji, Kyoto 611-0011, Japan, and Laboratory of Quality Design of Exploitation, Division of Agronomy and Horticultural Science, Graduate School of Agriculture, Kyoto University, Uji, Kyoto 611-0011, Japan

Received October 18, 2004; Revised Manuscript Received February 3, 2005

ABSTRACT: A Gram-negative bacterium, *Sphingomonas* sp. A1, has a macromolecule (alginate) import system consisting of a pit on the cell surface and an alginate-specific ATP-binding cassette importer in the inner membrane. Transport of alginate from the pit to the ABC importer is probably mediated by two periplasmic binding protein homologues (AlgQ1 and AlgQ2). Here we describe characteristics of binding of AlgQ1 and AlgQ2 to alginate and its oligosaccharides through surface plasmon resonance biosensor analysis, UV absorption difference spectroscopy, and X-ray crystallography. Both AlgQ1 and AlgQ2 were inducibly expressed in the periplasm of alginate-grown cells of strain A1. Biosensor analysis indicated that both proteins specifically bind alginate with a high degree of polymerization (>100) and that dissociation constants for alginate with an average molecular mass of 26 kDa are 2.3×10^{-7} M for AlgQ1 and 1.5×10^{-7} M for AlgQ2. An in vitro ATPase assay using the membrane complex, including the alginate ABC importer, suggested that both alginate-bound forms of AlgQ1 and AlgQ2 are closely associated with the importer. X-ray crystallography showed that AlgQ1 consisted of two domains separated by a deep cleft that binds alginate oligosaccharides through a conformational change in the two domains. These results directly show that alginate-binding proteins play an important role in the efficient transport of alginate macromolecules with different degrees of polymerization in the periplasm.

Alginate is a linear polysaccharide composed of α-L-guluronate (G)[1] and its C5 epimer *β*-D-mannuronate (M), arranged in three different ways: poly-α-L-guluronate (polyG), poly-*β*-D-mannuronate (polyM), and heteropolymeric random sequences (polyMG) (*1*). Alginate produced by brown seaweed is widely used in the food and pharmaceutical industries because the polymer chelates metal ions and forms a highly viscous solution (*2*).

Sphingomonas sp. A1 (strain A1) isolated from soil is a Gram-negative bacterium assimilating a macromolecule (alginate) (*3*), and directly incorporates the polymer into cytoplasm through a biosystem consisting of a mouthlike pit on the cell surface and an alginate-specific ATP-binding cassette (ABC) transporter in the inner membrane (*4*, *5*). Incorporated alginate is depolymerized to constituent monosaccharides through the reactions of three endotype alginate lyases (A1-I, A1-II, and A1-III) and one exotype alginate lyase (A1-IV) in the cytoplasm (*6*, *7*).

ABC transporters typically consist of four subunits (two ABC proteins and two transmembrane subunits) (*8*), and are classified into two groups, importers and exporters, on the basis of the direction of solute flow. Almost all ABC importers from bacteria to mammals analyzed thus far transport small molecules with a molecular mass of less than 2 kDa such as sugars, amino acids, oligopeptides, metals, anions, iron chelators (siderophores), and vitamin B_{12} (*8*). In macromolecule assimilation, living cells generally incor-

[†] This work was supported in part by grants-in-aid from the Ministry of Education, Culture, Sports, Science and Technology of Japan to K. Murata (16013221, 15013228, and 14360052) and W.H. (15780053), by a grant of the National Project on Protein Structure and Functional Analysis from the Ministry of Education, Culture, Sports, Science and Technology of Japan to B.M., and by a grant from the Japan Society for the Promotion of Science to Y.M. (03619). This work was further supported in part by the Program for Promotion of Basic Research Activities for Innovative Biosciences (PROBRAIN) of Japan.

[‡] The atomic coordinates and protein factors have been deposited in the Protein Data Bank as entries 1Y3Q for apo-AlgQ1, 1Y3P for holo-AlgQ1-TE, and 1Y3N for holo-AlgQ1-DI.

* To whom correspondence should be addressed. Telephone: +81-774-38-3766. Fax: +81-774-38-3767. E-mail: kmurata@kais.kyoto-u.ac.jp.

[§] Division of Food Science and Biotechnology.

[||] Division of Agronomy and Horticultural Science.

[⊥] These authors contributed equally to this work.

[1] Abbreviations: G, α-L-guluronate; M, *β*-D-mannuronate; polyG, poly-α-L-guluronate; polyM, poly-*β*-D-mannuronate; polyMG, heteropolymer consisting of G and M; strain A1, *Sphingomonas* sp. A1; ABC, ATP-binding cassette; A1-I, strain A1 alginate lyase I; A1-II, strain A1 alginate lyase II; A1-III, strain A1 alginate lyase III; A1-IV, strain A1 alginate lyase IV; AlgQ1, strain A1 periplasmic alginate-binding protein; AlgQ2, strain A1 periplasmic alginate-binding protein; AlgS, strain A1 ABC protein for alginate import; AlgM1, strain A1 transmembrane domain for alginate import; AlgM2, strain A1 transmembrane domain for alginate import; KPB, potassium phosphate buffer; DTT, dithiothreitol; SPR, surface plasmon resonance; RU, resonance units; rms, root-mean-square; MalE, *E. coli* periplasmic maltose-binding protein; MalK, *E. coli* ABC protein for maltose import; MalF, *E. coli* transmembrane domain for maltose import; MalG, *E. coli* transmembrane domain for maltose import; WAT, water molecule.

10.1021/bi047781r CCC: $30.25
Published on Web 03/10/2005

porate small molecules produced by extracellular macromolecule-degrading enzymes. The alginate ABC importer of strain A1 is thus unusual in that the substrate is a macromolecule with an average molecular mass of 26 kDa. In most ABC importers in Gram-negative bacteria such as *Escherichia coli* (*9*), a periplasmic binding protein mediates the transport of the substrate from the outer membrane to an ABC importer in the inner membrane, and genes encoding the binding protein and ABC importer are assembled into a cluster (*10*). A system consisting of ABC proteins, transmembrane domains, and an associated periplasmic binding protein thus is crucial for substrate import. This is also true in the ABC importer system for alginate in strain A1; i.e., the strain A1 genetic cluster for the alginate import system contains five genes for an ABC protein (AlgS), transmembrane domains (AlgM1 and AlgM2), and two binding proteins (AlgQ1 and AlgQ2), in that order (*5*). Although the alginate ABC importer of strain A1 has a general architecture composed of two molecules of AlgS and a heterodimer of AlgM1 and AlgM2, the organization of the genetic cluster for the alginate import system is unusual in that it contains two copies of binding proteins. In *E. coli*, 44 ABC importers are estimated to be encoded in the genome, and almost all have one type of ABC importer-associated periplasmic binding protein except for the arginine ABC importer (ArtP, ArtM, and ArtQ system) and the putative ABC importer (YrbF and YrbE system) (*9*).

We have recently determined the crystal structures of AlgQ2 and its complex with alginate tetrasaccharide by X-ray crystallography (*11*, *12*). AlgQ2 consists of two domains separated by a cleft, and binds and releases alginate tetrasaccharide through the conformational change in the two domains. No direct evidence shows, however, that proteins (AlgQ1 and AlgQ2) are expressed in the periplasm of strain A1 cells and bind alginate macromolecules. Structural and functional differences between AlgQ1 and AlgQ2 remain to be clarified, although primary structures of both proteins are similar (76% identical). This article clarifies the expression of AlgQ1 and AlgQ2 in strain A1, their interaction with the alginate ABC importer, and their characteristics in binding to macromolecules and oligosaccharides. Our results provide new insights into the bacterial molecular mechanism underlying macromolecule import in periplasm.

EXPERIMENTAL PROCEDURES

Materials. Alginate (sodium salt; average molecular mass of 26 kDa; D-mannuronate, 56.5%) from *Eisenia bicyclis* and hyaluronate (sodium salt) were purchased from Nacalai Tesque Inc. (Kyoto, Japan). PolyM (M, 95.1%; G, 4.9%) and polyG (M, 6.1%; G, 93.9%) were kindly donated by T. Sawabe (Hokkaido University, Hokkaido, Japan). CM-Toyopearl 650M, DEAE-Toyopearl 650M, and SuperQ-Toyopearl 650C were purchased from Tosoh Corp. (Tokyo, Japan). Restriction endonucleases were obtained from Takara Bio Inc. (Otsu, Japan) and DNA-modifying enzymes from Toyobo Co., Ltd. (Tokyo, Japan). Gellan (average molecular mass of 500 kDa, deacetylated) and pectin (average molecular mass of 350 kDa) were purchased from Wako Pure Chemical Industries, Ltd. (Osaka, Japan). Pyruvylated xanthan (average molecular mass of 2000 kDa) was a gift from Kohjin Co., Ltd. (Tokyo, Japan).

Microorganisms and Culture Conditions. To assess the expression of binding proteins and prepare the membrane complex, strain A1 cells were cultured aerobically at 30 °C in an alginate medium consisting of 0.1% $(NH_4)_2SO_4$, 0.1% KH_2PO_4, 0.1% Na_2HPO_4, 0.01% $MgSO_4 \cdot 7H_2O$, 0.01% yeast extract, and 0.5% alginate (pH 7.2) or a glucose medium containing 0.5% glucose in place of alginate (pH 7.2). *E. coli* strains HMS174(DE3)pLysS and BL21(DE3)pLysS (Novagen, Madison, WI) were used as hosts for overexpression of AlgQ1 and AlgQ2, respectively. For expression of proteins in *E. coli*, cells were precultured aerobically at 37 °C in Luria-Bertani (LB) medium (*13*) supplemented with ampicillin (0.1 mg/mL). When the turbidity reached 0.5 at 600 nm, isopropyl β-D-thiogalactopyranoside was added to the culture (1 mM), and cells were further cultured at 16 °C for 12 h.

Isolation of Periplasmic Fractions. Periplasmic fractions were separated from exponentially and stationary growing cells of strain A1 on alginate or glucose as described elsewhere (*14*). Unless otherwise specified, all procedures were conducted at 0−4 °C. Briefly, strain A1 cells (wet weight of 7 g) were collected by centrifugation at 6000*g* and 4 °C for 5 min, washed with distilled water, and then resuspended in distilled water (26 mL). After the addition of 0.1 M Tris-HCl (pH 8.3) (15.7 mL), 2 M sucrose (13.2 mL), 1% EDTA (2.6 mL), and 0.5% lysozyme (2.6 mL), the cell suspension was incubated at 30 °C for 1 h and then centrifuged at 20000*g* for 15 min. The supernatant was ultracentrifuged at 100000*g* for 1 h. The resulting supernatant was dialyzed against 20 mM Tris-HCl (pH 7.5) and the dialysate used as a periplasmic fraction.

Sequencing and Manipulation of DNA. The AlgQ1 gene nucleotide sequence was determined by dideoxy chain termination using a model 377 automated DNA sequencer (Applied Biosystems Division of Perkin-Elmer, Foster City, CA) (*15*). Subcloning, transformation, and gel electrophoresis were conducted as described elsewhere (*13*).

Construction of the Plasmid for Overexpression of AlgQ1. An overexpression system for AlgQ1 was constructed in *E. coli* cells as follows. To introduce the AlgQ1 gene into an expression vector, pET3a (Novagen), PCR was conducted using KOD polymerase (Toyobo Co., Ltd.), the genomic DNA of strain A1 as a template, and two synthetic oligonucleotides as primers. Oligonucleotides for overexpression of AlgQ1 were 5′-TCTCCATATGTTCGCGGCTCCGTCGGTG-3′ and 5′-CCGGATCCTTACTTGGCTCCGACCTGGGCTG-3′, with *Nde*I and *Bam*HI sites (underlined) added to their 5′ regions. The fragment amplified through PCR was digested with *Nde*I and *Bam*HI and then ligated with *Nde*I- and *Bam*HI-digested pET3a. The resultant plasmid containing the AlgQ1 gene was designated pAQ1.

Protein Assay. Protein concentrations were determined by the method of Bradford (*16*), with bovine serum albumin as the standard.

Purification of AlgQ1 and AlgQ2 from Cells of E. coli. Unless otherwise specified, all procedures were conducted at 0−4 °C. Cells of *E. coli* strain HMS174(DE3)pLysS harboring pAQ1 were grown in 1 L of LB medium (1 L/flask), collected by centrifugation at 6000*g* and 4 °C for 5 min, washed with 20 mM potassium phosphate buffer (KPB) (pH 6.8), and then resuspended in the same buffer. Cells were ultrasonically disrupted (model 201M insonator,

Kubota, Tokyo, Japan) at 0 °C and 9 kHz for 20 min, and the clear solution obtained upon centrifugation at 15000*g* and 4 °C for 20 min was used as a cell extract. The cell extract was applied to a CM-Toyopearl 650M column (2.6 cm × 10 cm) previously equilibrated with 20 mM KPB (pH 6.8). The protein was eluted with a linear gradient of 0 to 0.5 M NaCl (300 mL) in 20 mM KPB (pH 6.8), with a 3 mL fraction collected every 3 min. Fractions containing AlgQ1, eluted with 0.3−0.4 M NaCl, were combined and dialyzed against 20 mM sodium HEPES (pH 6.8). The dialysate was used as a purified AlgQ1. AlgQ2 was also purified from cells of *E. coli* strain BL21(DE3)pLysS harboring pAQ2 as described elsewhere (*11*).

Preparation of anti-AlgQ2 Antibodies and Western Blotting. AlgQ2 purified from cells of *E. coli* was injected into a rabbit to raise anti-AlgQ2 antibodies. After the rabbit was bled, antiserum was obtained by centrifugation and used as anti-AlgQ2 antibodies. To determine the expression of binding proteins in strain A1, bacterial cells and their periplasmic fractions were subjected to SDS−PAGE (*17*), followed by Western blotting using anti-AlgQ2 antibodies as described elsewhere (*18*). Anti-IgG conjugated with horseradish peroxidase (Pharmacia Biotech, Uppsala, Sweden) and a POD Immunostain system (Wako Pure Chemical Industries, Ltd.) were used to visualize the cross reaction.

N-Terminal Amino Acid Sequence. The N-terminal amino acid sequence of AlgQ1 purified from *E. coli* cells was determined by Edman degradation with a Procise 492 protein sequencing system (Applied Biosystems Division of Perkin-Elmer).

Biosensor Analysis of Alginate Binding by AlgQ1 and AlgQ2. Surface plasmon resonance (SPR) biosensor analysis was conducted at 25 °C using CM5 sensor chips on a Biacore 3000 instrument (Biacore International AB, Uppsala, Sweden). AlgQ1 and AlgQ2 were each immobilized in the dextran matrix on a CM5 sensor chip through amino coupling. Dextran surfaces of flow cells on the chip were activated with a mixture (35 μL) of *N*-ethyl-*N*′-(dimethylaminopropyl)carbonate (750 mg/mL) and *N*-hydroxysuccinimide (115 mg/mL), and then reacted with the protein (45 μg/mL, 35 μL) in 10 mM sodium acetate (pH 4.0) at a flow rate of 5 μL/min. Unreacted activated dextran surfaces were blocked with 1 M ethanolamine (35 μL) at the same flow. Five types of 10 mM buffers containing 150 mM NaCl and 0.005% Tween 20, i.e., sodium acetate (pH 4.0), sodium acetate (pH 5.0), MES-NaOH (pH 6.0), HBS-EP (pH 7.4) (10 mM HEPES and 3 mM EDTA), and Tris-HCl (pH 8.0), were used as dilution and running buffers. Alginate diluted to different concentrations (0.26−6.5 mg/mL) was injected over AlgQ1- or AlgQ2-immobilized surfaces at a flow rate of 20 μL/min, and binding after 2 min injections was assessed in resonance units (RU). After alginate was injected, the running buffer was let to flow for dissociation at the same flow. Tris-HCl (0.1 M, pH 8.0) was used to regenerate the sensor chip. To determine substrate specificity in the binding assay, pectin, xanthan, gellan, and hyaluronate were used instead of alginate. All binding data were subtracted from data for binding to a blank flow cell.

Preparation of Alginate Oligosaccharides. To determine the substrate specificity of AlgQ1 and AlgQ2, polyM and polyG were depolymerized by alginate lyases (A1-III and A1-II) into di- and tetrasaccharides, respectively (*6*). Alginate di- and tetrasaccharides for cocrystallization were prepared by reacting alginate with alginate lyase A1-III (*19*). Alginate oligosaccharides were purified by gel permeation column chromatography (Bio-Gel P2, Bio-Rad, Richmond, CA).

UV Absorption Difference Spectroscopy. UV absorption difference spectra observed in interactions between proteins (AlgQ1 and AlgQ2) and sugars (alginate oligosaccharides) were examined at pH 7.0 (10 mM sodium HEPES) with a Shimadzu MPS-2000 spectrophotometer at 25 °C.

Partial Purification of the Membrane Complex. The membrane complex containing the alginate ABC importer was detected by Western blotting using anti-AlgS antibodies as described elsewhere (*5*). Cells of strain A1 cultured in 300 L of alginate medium at 30 °C for 48 h were harvested by centrifugation, washed once with 50 mM Tris-H_2SO_4 (pH 8.0) containing 1 mM EDTA, and resuspended in the same buffer. They were then lysed in the presence of DNase by two sonication passes. After removal of unbroken cells by centrifugation at 3000*g* and 4 °C for 10 min, the resultant supernatant was transferred to a clean tube. The centrifugation step was repeated twice. The supernatant was subjected to ultracentrifugation at 100000*g* and 4 °C for 1 h. The membrane pellet was washed with 50 mM Tris-H_2SO_4 (pH 8.0) and subjected to a second ultracentrifugation at 100000*g* and 4 °C for 1 h. The final pellet was resuspended in 50 mM Tris-H_2SO_4 (pH 8.0) at a protein concentration of 15 mg/mL and frozen in aliquots at −80 °C. Membrane vesicles, prepared as described above (15 mg/mL, typically 350 mg total), were incubated with 1.5 volumes of 10 M urea for 10 min on ice and collected by ultracentrifugation at 100000*g* and 4 °C for 30 min. The pellet was washed once with 20 mM Tris-H_2SO_4 (pH 8.0) and resuspended at a protein concentration of 2.5 mg/mL in buffer containing 20 mM Tris-H_2SO_4 (pH 8.0), 5 mM $MgCl_2$, 1 mM dithiothreitol (DTT), and 20% glycerol. Proteins were solubilized from urea-treated membranes by addition of 1.2% octyl glucoside. After incubation on ice for 20 min, the particulate fraction was removed by ultracentrifugation at 100000*g* and 4 °C for 30 min. The supernatant was loaded onto a DEAE-Toyopearl 650M column (1.2 cm × 6 cm) previously equilibrated with buffer A containing 20 mM Tris-H_2SO_4 (pH 8.0), 1 mM DTT, 20% glycerol, and 0.2% octyl glucoside. The column was washed with 10 mL of buffer A and then eluted with a linear gradient of 0 to 0.5 M Na_2SO_4 in buffer A (30 mL) at a flow rate of 0.5 mL/min, a 1 mL fraction being collected every 1 min. Desired fractions containing AlgS were dialyzed against buffer B containing 50 mM Tris-H_2SO_4 (pH 7.5), 50 mM Na_2SO_4, 1 mM DTT, 20% glycerol, and 0.2% octyl glucoside, applied to a SuperQ-Toyopearl 650C column (1.2 cm × 5 cm) previously equilibrated with buffer B, and eluted with a linear gradient of 0 to 0.5 M Na_2SO_4 in buffer B (30 mL) at a flow rate of 0.5 mL/min, a 1 mL fraction being collected every 1 min. Fractions containing AlgS, eluted with 0.3 M Na_2SO_4, were dialyzed against buffer B, and the dialysate was used as a partially purified membrane complex containing the alginate ABC importer.

ATPase Assay. ATPase activity was measured as described elsewhere (*5*). The final concentrations of the membrane complex, AlgQ1, AlgQ2, AlgS, and alginate in the assay mixture were 5 mg/mL, 2 mg/mL, 2 mg/mL, 1 mg/mL, and 1.0 mM, respectively.

Crystallization and X-ray Diffraction. Crystals of apo-AlgQ1 (ligand-free) were obtained by hanging-drop vapor diffusion. The solution for a crystallization drop was prepared at 20 °C on a siliconized cover slip by mixing 3 μL of the protein solution (15 mg/mL) with an equal volume of mother liquor consisting of 30% polyethylene glycol 4000, 0.1 M $MgCl_2$, and 0.1 M Tris-HCl (pH 8.5). Cocrystals of AlgQ1 with alginate oligosaccharides were obtained in the same way. The mother liquor for cocrystallization consisted of 20% polyethylene glycol 8000, 1 mM alginate di- or tetrasaccharide, and 0.1 M sodium citrate (pH 5.6). Diffraction data for crystals of AlgQ1 were collected up to 1.9 Å for apo-AlgQ1, 2.0 Å for tetrasaccharide-bound AlgQ1 (holo-AlgQ1-TE), and 1.6 Å for disaccharide-bound AlgQ1 (holo-AlgQ1-DI), with a λ of 0.9 Å, using an Oxford PX210 CCD detector at beamline BL44XU (Beamline for Macromolecule Assemblies, Institute for Protein Research, Osaka University, Osaka, Japan) at SPring-8 (Hyogo, Japan). Data were collected at the temperature of liquid nitrogen. A complete data set was recorded for a single crystal with exposure of 8 s for a 1° oscillation. Collected images were processed with D*Trek (*20*) and CCP4 truncate (*21*).

Structure Determination and Refinement. Crystal structures of AlgQ1 and its complexes with sugars were determined by molecular replacement using CNS-SOLVE (*22*). Coordinates of the ligand-free form of AlgQ2 (*11*) [apo-AlgQ2; RCSB Protein Data Bank entry 1KWH (*23*)] were used as a search model. The model was built with TURBO-FRODO (Bio-Graphics) on a Silicon Graphics Octane computer. Annealing refinement was simulated with this model using 15−2.5 Å resolution data. $|F_o| - |F_c|$ and $2|F_o| - |F_c|$ maps were used to locate the correct model. Several rounds of conjugate gradient minimization refinement and *B*-factor refinement, followed by manual model building, were carried out to improve the model by increasing data to 1.9, 2.0, and 1.6 Å resolution for apo-AlgQ1, holo-AlgQ1-TE, and holo-AlgQ1-DI, respectively. Water molecules were incorporated when the difference in density exceeded 3.0σ above the mean, and the $2|F_o| - |F_c|$ map showed a density exceeding 1.0σ. The stereo quality of the model was assessed using PROCHECK (*24*). Molecular models were superimposed using the fitting program included in TURBO-FRODO (Bio-Graphics). Ribbon plots were prepared using MOLSCRIPT (*25*) and RASTER3D (*26*).

RESULTS

Expression of AlgQ1 and AlgQ2 in Cells of Strain A1. The expression of AlgQ1 and AlgQ2 in strain A1 cells was investigated by Western blotting using anti-AlgQ2 antibodies (Figure 1). Cells grown on alginate appeared to produce only AlgQ2 (Figure 1, lane 4), although neither AlgQ1 nor AlgQ2 was detected in cells grown on glucose (data not shown). Primary structure-based analysis using PSORT (http://www.psort.org/) and ProtScale (http://kr.expasy.org/tools/protscale.html) predicted both to be soluble secretory proteins with signal peptides, suggesting that they are periplasmic proteins. In fact, the N-terminal sequence of AlgQ1 purified from *E. coli* cells was determined to be ^{25}REATW^{29}, and both AlgQ1 and AlgQ2 expressed in *E. coli* cells were localized in the periplasm, indicating that the first 24 amino acid residues should function as a signal peptide as with AlgQ2 (*11*). Periplasmic fractions from exponentially and stationary growing cells of strain A1 on alginate were subjected to Western blotting and found to contain both AlgQ1 and AlgQ2 (Figure 1, lanes 5 and 6). The absence of AlgQ1 protein bands in alginate-grown cells (lane 4) was probably due to the limited amount of cells applicable to Western blotting. No proteins cross-reacting with anti-AlgQ2 antibodies were observed in periplasmic fractions from cells grown on glucose (Figure 1, lanes 7 and 8), indicating that AlgQ1 and AlgQ2 are periplasmic proteins that can be induced in the presence of alginate.

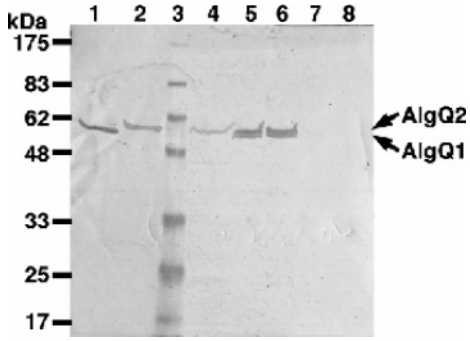

FIGURE 1: Expression of strain A1 AlgQ1 and AlgQ2. SDS−PAGE, followed by Western blotting using anti-AlgQ2 antibodies: lane 1, purified AlgQ1 (0.5 μg of protein); lane 2, purified AlgQ2 (0.5 μg of protein); lane 3, molecular mass standards (from the top, 175, 83, 62, 48, 33, 25, and 17 kDa); lane 4, cells of strain A1 grown on alginate; lane 5, periplasmic fraction of exponentially growing cells of strain A1 on alginate; lane 6, periplasmic fraction of stationary growing cells of strain A1 on alginate; lane 7, periplasmic fraction of exponentially growing cells of strain A1 on glucose; and lane 8, periplasmic fraction of stationary growing cells of strain A1 on glucose.

Binding of AlgQ1 and AlgQ2 to Alginates. The SPR biosensor is powerful in analyzing the macromolecule interactions by detecting mass changes accompanying the binding of a soluble analyte to a ligand immobilized in the dextran matrix on the sensor chip. To assess interactions between proteins (AlgQ1 and AlgQ2) and the macromolecular polysaccharide through SPR biosensor analysis, AlgQ1 and AlgQ2 purified from *E. coli* cells were immobilized in the dextran matrix on the sensor chip at 11 338 and 10 246 RU, respectively. Initial experiments conducted using alginate dissolved in the general running buffer, HBS-EP (pH 7.4), showed interactions between proteins (AlgQ1 and AlgQ2) and alginate that increased in frequency with an increase in alginate concentration (Figure 2a,b). Part of the alginate once bound to AlgQ1 and AlgQ2 was dissociated by the running buffer flow. Although multiple binding data cannot be fitted completely to the 1:1 binding models provided with BIAevaluation (Biacore International AB), dissociation constants (K_d) between proteins and alginate were estimated to be 6 μg/mL for AlgQ1 and 4 μg/mL for AlgQ2, which correspond to 0.23 and 0.15 μM, respectively, when alginate with an average molecular mass of 26 kDa was used (Table 1). Since profiles of binding of AlgQ1 to alginate were similar to those of AlgQ2, results are shown below for only AlgQ1. The effects of pH (4.0−8.0) on the interaction were then examined. The binding of AlgQ1 to alginate was detected when buffers at pH 4.0, 5.0, and 6.0 were used, and peaked at pH 4.0 (Figure 2c). No interaction was observed at pH 8.0. AlgQ1 bound alginate and xanthan, but with greater affinity for alginate (Figure 2d). Alginates with different degrees of polymerization (100−500) became

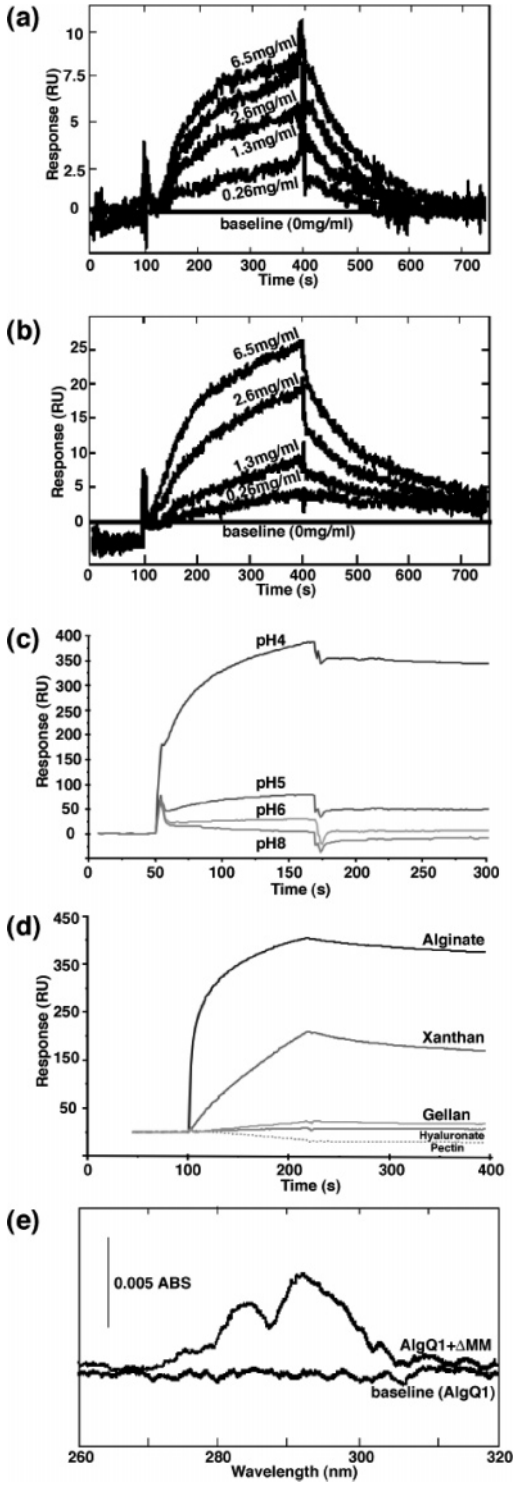

FIGURE 2: AlgQ1 and AlgQ2 binding to poly- and oligosaccharides. Interaction between proteins and polysaccharides and between proteins and oligosaccharides was studied by SPR biosensor analysis (a−d) and UV absorption difference spectroscopy (e). (a) Dependence of alginate concentration (0.26, 1.3, 2.6, and 6.5 mg/mL) on AlgQ1 binding to alginate at pH 7.4. (b) Dependence of alginate concentration (0.26, 1.3, 2.6, and 6.5 mg/mL) on AlgQ2 binding to alginate at pH 7.4. (c) Effect of pH on AlgQ1 binding to alginate. Alginates (1 mg/mL) dissolved in different buffers were injected over AlgQ1-immobilized surfaces: pH 4.0, sodium acetate; pH 5.0, sodium acetate; pH 6.0, MES-NaOH; and pH 8.0, Tris-HCl. (d) Specificity in AlgQ1 binding to 100 μg/mL polysaccharides (alginate, xanthan, gellan, hyaluronate, and pectin) at pH 4.0. (e) UV absorption difference spectrum observed on binding of AlgQ1 (1.7 μM) and alginate disaccharide (ΔMM) (20 μM) at pH 7.0 and 25 °C.

Table 1: Dissociation Constants between Alginate-Binding Proteins and Sugars

substrate	dissociation constant K_d (μM) AlgQ1	AlgQ2
alginate	0.23[a]	0.15[a]
disaccharide ΔMM[b]	2.8	6.1
alginate tetrasaccharide[c]	15	13
G-rich alginate tetrasaccharide[d]	9.1	14
maltose	ND[e]	ND[e]

[a] Calculated using the average molecular mass of 26 kDa. See the text for details. [b] PolyM depolymerized to disaccharide through the A1-III reaction. [c] Same sample that was used for cocrystallization. [d] G-rich alginate tetrasaccharide produced from polyG through the A1-II reaction. [e] A 0.83 mM substrate solution gave no difference in the UV spectrum.

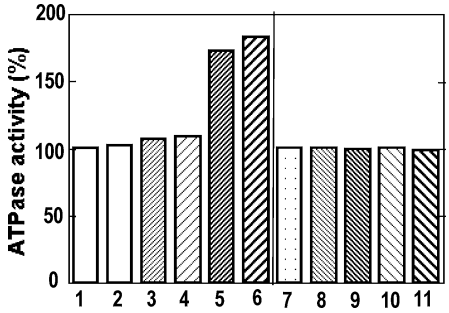

FIGURE 3: ATPase activity of the membrane complex: lane 1, membrane complex alone; lane 2, membrane complex with alginate; lane 3, membrane complex with AlgQ1; lane 4, membrane complex with AlgQ2; lane 5, membrane complex with AlgQ1 and alginate; lane 6, membrane complex with AlgQ2 and alginate; lane 7, purified AlgS alone; lane 8, purified AlgS with AlgQ1; lane 9, purified AlgS with AlgQ2; lane 10, purified AlgS with AlgQ1 and alginate; and lane 11, purified AlgS with AlgQ2 and alginate. The ATPase activity of the membrane complex is 0.08 μmol min^{-1} (mg of protein)$^{-1}$ and that of AlgS alone 0.88 μmol min^{-1} (mg of protein)$^{-1}$, both of which are taken relatively to be 100%.

substrates for AlgQ1 and AlgQ2 (data not shown), while other polysaccharides such as pectin, gellan, and hyaluronate were inert as substrates (Figure 2d), indicating that AlgQ1 and AlgQ2 are specific to alginate.

Interactions of AlgQ1 and AlgQ2 with oligo- and monosaccharides were analyzed using UV absorption difference spectroscopy. Spectral changes were observed when alginate oligosaccharides were added to the protein solution (Figure 2e). Since differences depending on the substrate concentration gave a saturation curve, dissociation constants (K_d) were determined to be 2.8−15 μM for alginate oligosaccharides by nonlinear curve fitting (Table 1). No significant difference in K_d was seen between AlgQ1 and AlgQ2 for alginate oligosaccharides. Although results through UV absorption difference spectroscopy suggest that both proteins interact specifically with alginate oligosaccharides in addition to the macromolecule alginate, further analysis was required for the direct evidence regarding interactions between proteins and oligosaccharides.

Interaction of AlgQ1 and AlgQ2 with the Membrane Complex. Since AlgQ1 and AlgQ2 were identified as macromolecule-binding (alginate-binding) proteins localized in periplasm, we studied their association with the alginate ABC importer contained in the membrane complex (Figure 3). Through SDS−PAGE analysis followed by staining with Coomasie brilliant blue and Western blotting using anti-AlgS

Table 2: Data Collection and Refinement Statistics

	apo-AlgQ1	holo-AlgQ1-TE	holo-AlgQ1-DI
crystal			
space group	$P2_12_12_1$	$P2_1$	$P2_1$
cell dimensions [a (Å), b (Å), c (Å), β (deg)]	49.2, 59.2, 165.3	58.8, 67.4, 63.0, 95.9	58.5, 67.8, 62.8, 95.3
no. of molecules/asymmetric unit	1	1	1
data collection			
no. of measured reflections	229676	135158	314762
no. of unique reflections	41719	33209	63420
R_{sym} (%)	9.4	10.1	9.4
completeness	99.7	99.0	99.5
refinement			
resolution (Å)	8−1.9	15−2.0	15−1.6
no. of reflections used	38345 (99.7%)	32534 (98.1%)	63331 (97.4%)
no. of residues/no. of waters	490/326	490/406	490/654
no. of calcium ions	1	1	1
saccharide	−	one tetramer	one dimer
average *B*-factor	20.4	19.1	16.2
structure form	open	closed	closed
rms deviation			
bond lengths (Å)	0.0077	0.0056	0.0051
bond angles (deg)	1.38	1.24	1.25
R-factor (%)	19.4	19.9	19.7
R_{free} (%)	24.4	25.5	22.4

antibodies, we confirmed that the partially purified complex included the alginate ABC importer as major proteins and the other proteins as a few faint proteins. The complex exhibited ATPase activity, the level of which did not change in the presence of alginate (Figure 3, lanes 1 and 2). Activity in the complex was slightly elevated in the presence of ligand-free alginate-binding proteins (Figure 3, lanes 3 and 4), while alginate-bound proteins significantly increased enzyme activity (Figure 3, lanes 5 and 6). AlgS was purified by further purification of the membrane complex that constitutes a homodimer and exhibits ATPase activity, which was not activated even in the presence of alginate-bound proteins (Figure 3, lanes 10 and 11). These data suggest that the activation of AlgS by alginate-bound AlgQ1 and AlgQ2 is mediated through transmembrane domains, although these experiments were still primitive because of the possibility that the membrane complex might contain a faint ATPase other than AlgS.

Structure Determination of AlgQ1 and Its Complexes with Di- and Tetrasaccharides. To clarify the structural difference between AlgQ1 and AlgQ2, and to obtain direct evidence of interactions between proteins and oligosaccharides, crystal structures of AlgQ1 and its complexes with alginate di- and tetrasaccharides were determined by X-ray crystallography. Table 2 summarizes the results of X-ray data collection and refinement statistics. All models of AlgQ1 (apo and holo forms) consist of 490 amino acids, suggesting that proteins are truncated. In fact, the C-terminal amino acid was determined to be Tyr by carboxypeptidase Y digestion and amino acid analysis, indicating that AlgQ1 was digested between Tyr490 and Gly491. The polypeptide chain sequence for the 490 amino acids was well traced, and the electron density of main and side chains was generally very well defined on the $2|F_o| - |F_c|$ map. Judging from the results of Ramachandran plot analysis (*27*), we confirmed that most non-glycine residues lie within most favored regions, the exception being Lys251 (apo-AlgQ1, $\phi = 65°$ and $\psi = -141°$; holo-AlgQ1-TE, $\phi = 62°$ and $\psi = -133°$; and holo-AlgQ1-DI, $\phi = 65°$ and $\psi = -139°$), which is present in a generously allowed region. Lys251 is located next to the terminus of a helix (H12/C). The $2|F_o| - |F_c|$ density map exceeding 1.0σ was not strong enough to identify the reducing end sugar residue of holo-AlgQ1-TE, so we used the map exceeding 0.6σ and found a D-mannuronate α-anomer to be the best fit for the density map.

Figure 4a shows a ribbon model of apo-AlgQ1, which consists of two globular domains (N domain consisting of residues 1−133 and 310−400 and C domain consisting of residues 134−309 and 401−490) that form an α/β structure. These two domains are connected through three loop segments consisting of residues 133−136, 292−314, and 399−401. One calcium ion is present in the C domain. Overall structures of holo-AlgQ1-TE and holo-AlgQ1-DI are shown in panels b and c of Figure 4, respectively. Tetrasaccharide or disaccharide is bound in the deep cleft between the N and C domains.

Table 3 lists the root-mean-square (rms) deviation of equivalent Cα atoms calculated within a pair distance of 2.0 Å and altered rotation angle between N and C domains upon substrate binding. The rms difference between holo-AlgQ1-TE and holo-AlgQ1-DI for the entire structure is 0.42 Å, being 0.27 and 0.30 Å for the N and C domains, respectively. When N domains of apo and holo forms were superimposed, the rotation angle required to superimpose the C domain was determined to be 0.6°, so structures of holo-AlgQ1 with tetrasaccharide and disaccharide are almost the same. The rms difference between apo-AlgQ1 and holo-AlgQ1-TE is small for each N or C domain, and folding topologies of the N or C domain are similar. However, the value for the entire protein is larger, and the rotation angle was calculated to be 44°; the two domains are closer in holo-AlgQ1 because of substrate binding.

Alginate-Binding Sites. Binding sites of holo-AlgQ1-TE and holo-AlgQ1-DI are shown in Figure 5. The bound tetrasaccharide in holo-AlgQ1-TE is ribbon-shaped and consists of ΔM1-M2-G3-M4 from the nonreducing end, where ΔM, M, and G denote unsaturated D-mannuronate, saturated D-mannuronate, and saturated L-guluronate, respectively. Unsaturated mannuronate, ΔM1, was produced from alginate through the reaction of A1-III. Sugar-binding sites, corresponding to alginate residues, are designated S1−S4. Each alginate residue of the bound tetrasaccharide was in a

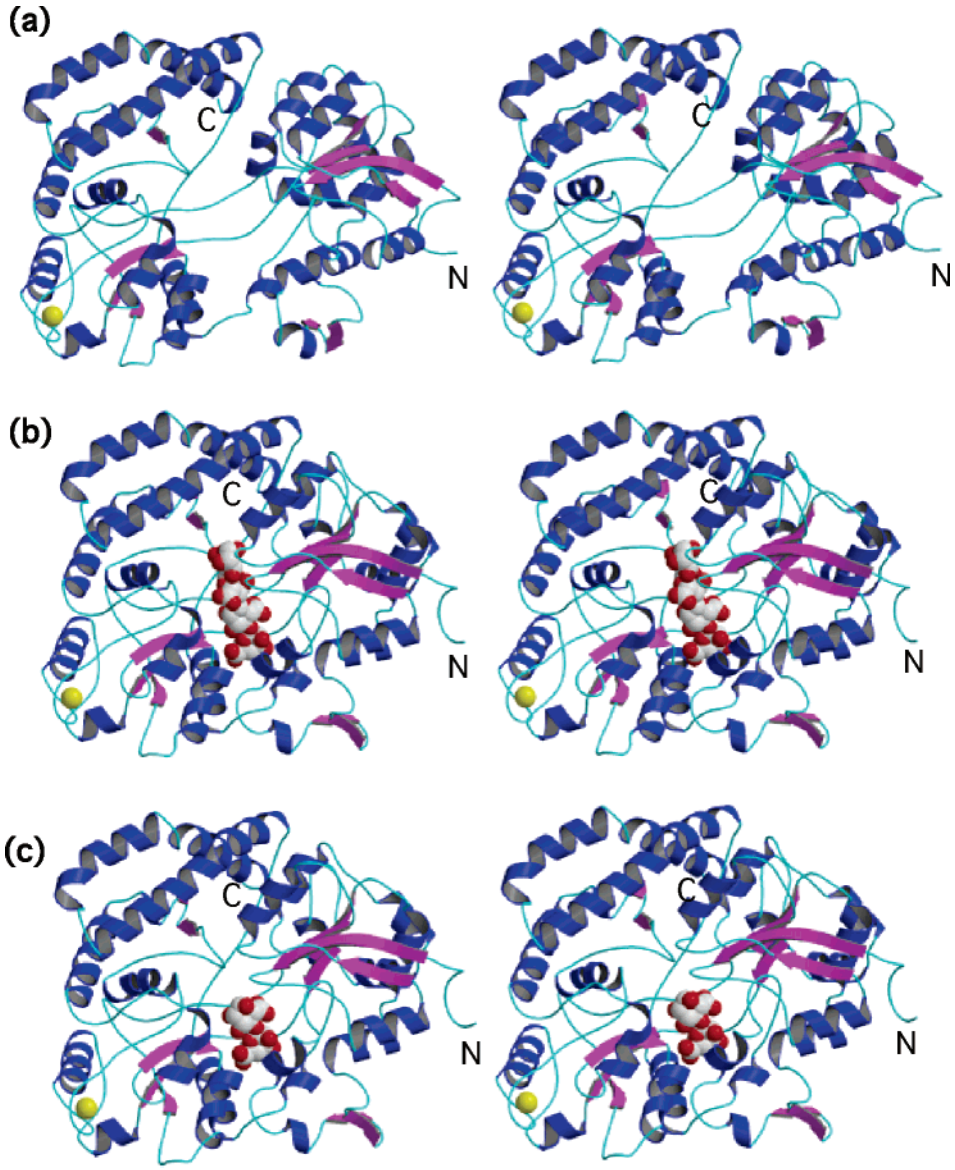

FIGURE 4: AlgQ1 structure: (a) apo-AlgQ1, (b) holo-AlgQ1-TE, and (c) holo-AlgQ1-DI. Colors denote secondary structure elements (blue for α-helices, purple for *β*-strands, cyan for loops and coils, and yellow for the calcium ion; sugar shown in CPK model). N marks the N-terminal end and C the C-terminal end.

Table 3: Comparison of Equivalent Domains and Rotation Angles

molecules compared[a]	rms difference for Cα atoms (Å)			altered rotation angle between the N and C domains (deg)
	entire structure	N domain	C domain	
holo-AlgQ1-TE vs holo-AlgQ1-DI	0.42 (490)	0.27 (216)	0.30 (247)	0.6
apo-AlgQ1 vs holo-AlgQ1-TE	1.53 (155)	0.39 (214)	0.54 (246)	44
apo-AlgQ2 vs holo-AlgQ2-TE[b]	1.45 (173)	0.63 (211)	0.59 (243)	33
apo-AlgQ1 vs apo-AlgQ2[c]	0.91 (463)	0.69 (212)	0.59 (246)	7
holo-AlgQ2-TE[b] vs holo-AlgQ1-TE	0.73 (487)	0.56 (214)	0.58 (246)	5

[a] The first molecule is open wider than the second. [b] Results for AlgQ2 complexed with tetrasaccharide (*12*). [c] Results for ligand-free AlgQ2 (*11*).

$^4C_1$ (M2 and M4) or $^1C_4$ pyranoside form (G3), and M1 is unsaturated mannuronate. In the holo-AlgQ1-DI crystal, bound disaccharide was found to consist of ΔM1-M2 with α-anomeric M2 at S1 and S2. The mode of binding to disaccharide ΔM1-M2 is the same as that in holo-AlgQ1-TE.

The bound oligosaccharides interact with surrounding amino acids. Table 4 summarizes hydrogen bond interactions between the bound alginate oligosaccharides and alginate-binding proteins. Secondary structure elements are designated the same as for apo-AlgQ2 (*11*). The number of direct hydrogen bonds between AlgQ1 and the tetrasaccharide in holo-AlgQ1-TE is 13 (ΔM1, 8; M2, 3; G3, 1; and M4, 1), and the number of associated water molecules is 13 (ΔM1, 2; M2, 6; G3, 3; and M4, 2). The number of direct hydrogen bonds between AlgQ1 and the disaccharide in holo-AlgQ1-

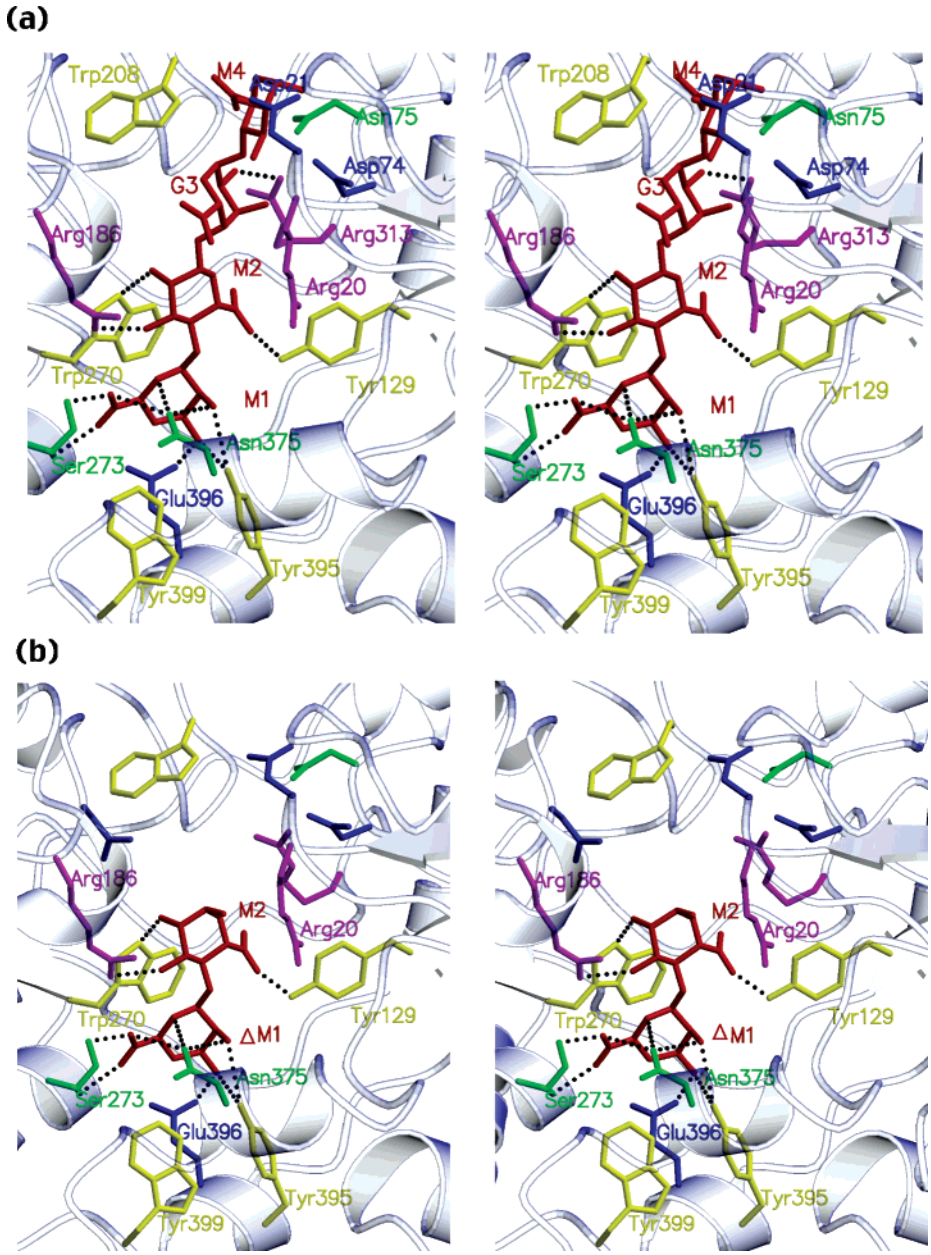

FIGURE 5: Binding site of holo-AlgQ1: (a) holo-AlgQ1-TE and (b) holo-AlgQ1-DI. Aromatic residues are colored yellow, basic residues pink, acidic residues cyan, and nonpolar residues green, and the sugar is colored red.

DI is 11 (ΔM1, 8; and M2, 3), and the number of associated water molecules is 10 (ΔM1, 2; and M2, 8). Hydrogen bond interactions between the disaccharide ΔM1-M2 and amino acid residues are almost the same in holo-AlgQ1-TE and holo-AlgQ1-DI, except for the M2−O1 interaction of the disaccharide reducing end in holo-AlgQ1-DI. Five water molecules are located at S3 and S4 subsites in holo-AlgQ1-DI. Table 5 summarizes C−C contacts between alginate oligosaccharides and alginate-binding proteins. The number of C−C contacts between AlgQ1 and tetrasaccharide holo-AlgQ1-TE is 36 (ΔM1, 23; M2, 7; G3, 2; and M4, 4). The number of C−C contacts between AlgQ1 and disaccharide holo-AlgQ1-DI is 30 (ΔM1, 23; and M2, 7). These results suggest that the nonreducing end of a sugar is heavily involved in binding with AlgQ1. C−C contacts are mainly through aromatic side chains, and the Trp270 residue in the C domain exhibits the most favorable stacking interactions with ΔM1. Most hydrogen-bonding residues are located in the N domain and most stacking aromatic residues in the C domain.

To analyze specificity at the S1 subsite, we used computational simulation to place saturated or unsaturated guluronate or saturated mannuronate at the S1 subsite. If saturated mannuronate is positioned thusly, O4 interacts with OE1 and OE2 of Glu396 at a distance of 2.8−2.9 Å. When guluronate is present instead of ΔM1, guluronate cannot form a C−C contact with Trp270 or other aromatic residues because both axial OH-2 and equatorial OH-3 of ΔM1 are displaced to the hydrophilic side.

Structural Comparison between AlgQ1 and AlgQ2. The overall structure of AlgQ1 is very similar to that of AlgQ2 (*11*, *12*). Some 24% of substitution is scattered over the sequence, but most residues that interact with alginate are conserved, except for residues 187 and 208. As shown in

Table 4: Hydrogen Bond Interactions between Alginate-Binding Proteins and Alginate Oligosaccharides

sugar atom	bond atom	element/domain	distance[a] (Å)/water number		
			holo-AlgQ1-TE	holo-AlgQ1-DI	holo-AlgQ2-TE[b]
ΔM1					
O2	Asn375 ND2	H18/N	3.2	3.2	3.2
O2	Tyr395 OH	H19/N	3.1	3.1	3.1
O2	water		2.7/WAT567	2.7/WAT625	2.8/WAT71
O3	Tyr395 OH	H19/N	3.0	2.9	2.9
O3	Glu396 OE1	H19/N	2.5	2.6	2.5
O5	Asn375 ND2	H18/N	2.9	3.1	3.1
O61	Asn375 ND2	H18/N	3.1	3.0	3.2
O61	Ser273 OG	H14/C	2.4	2.5	2.5
O62	water		2.7/WAT581	2.7/WAT612	2.8/WAT73
O62	Ser273 N	H14/C	2.9	3.0	3.0
M2					
O1	water	−	−	3.0/WAT621	−
O2	Trp270 NE1	SC2/C	3.4[c]	2.9	3.0
O2	water		3.3[c]/WAT652	2.8/WAT614	3.0/WAT973
O3	Arg186 NH2	L-SC1:H9/C	2.8	3.0	2.9
O4	water		2.9/WAT567	2.9/WAT625	2.9/WAT71
O5	water		3.1/WAT594	2.9/WAT616	−
O5	water		−	2.9/WAT1013	−
O61	water		2.7/WAT594	2.8/WAT597	2.7/WAT62
O61	water		2.7/WAT538	2.7/WAT616	2.7/WAT63
O62	Tyr129 OH	SA1/N	2.7	2.7	2.6
O62	water		2.7/WAT567	2.8/WAT625	2.8/WAT71
G3					
O2	Arg313 NH2	L-SC4:SA3/C−N	2.9		3.1
O2	water		3.1/WAT505		3.0/WAT276
O2	water		−		3.1/WAT86
O3	water		2.8/WAT852		2.9/WAT164
O61	water		3.2/WAT816		2.7/WAT380
O62	His187 NE2	L-SC1:H9/C	−		3.0
O62	water		−		2.8/WAT
M4					
O1	water		2.8/WAT576		2.7/WAT26
O1	water		−		2.8/WAT325
O2	Asp21 OD1	L-SA5:SA6/N	2.3		2.7
O3	water		−		3.1/WAT407
O61	water		−		2.7/WAT408
O61	water		−		2.8/WAT127
O62	water		2.8/WAT505		2.6/WAT580

[a] Distance of ≤3.2 Å. [b] Results for AlgQ2 molecule A (*12*). [c] More than 3.2 Å.

Table 3, apo-AlgQ1 is more open than apo-AlgQ2 (rotation angle of 7°), but holo-AlgQ1-TE is more closed than holo-AlgQ2-TE (rotation angle of 5°), which is the complex of AlgQ2 and alginate tetrasaccharide (*12*). The rotation angle of AlgQ1 upon substrate binding is therefore ∼10° greater than that of AlgQ2. Hydrogen bonds between N and C domains of apo- and holo-AlgQ1 are found in the same residues with AlgQ2 (*12*) (data not shown). Basically, the hinge bends in three connected loops (Table 6). Backbone torsion angles differ between AlgQ1 and AlgQ2 at residues 133, 134, and 310. In apo-AlgQ2, an indirect water-mediated hydrogen bond exists between the N of Gly133 and the O of Glu310 via a water molecule, and the hydrogen bond is lost in holo-AlgQ2-TE. In apo-AlgQ1, no indirect hydrogen bond exists between these residues because the O of Glu310 turns in the opposite direction due to substitution at residue 312 (Val in AlgQ2 to Pro in AlgQ1). This may be a reason for the difference in rotation angle between AlgQ1 and AlgQ2.

Even though tetrasaccharides used for cocrystallization are mixtures of M and MG blocks (*19*), we found ΔM1-M2-G3-M4 in both holo-AlgQ1-TE and holo-AlgQ2-TE with the same binding mode (Tables 4 and 5). This tetrasaccharide may be the predominant species, but AlgQ1 and AlgQ2 could recognize the same substrate.

Amino acid substitutions at alginate-binding sites consist of Asp187 and Trp208 in AlgQ1 to His187 and Tyr208 in AlgQ2. Interactions with ΔM1-M2 are the same in three holo forms, i.e., holo-AlgQ1-TE, holo-AlgQ1-DI, and holo-AlgQ2-TE. A C−C contact between M2 and Arg20 is found in holo-AlgQ1, whereas a C−C contact between M2 and His187 is found in holo-AlgQ2. At the S3 subsite, a hydrogen bond with His187 and a C−C contact with Arg313 are found in only holo-AlgQ2. A C−C bond exists between M4 and Trp208 in holo-AlgQ1-TE. The electron density map of M4 in holo-AlgQ1-TE is weaker than for other sugars, so M4 appears to be unstable at the S4 site.

DISCUSSION

We have directly demonstrated through SPR biosensor analysis that both AlgQ1 and AlgQ2 are macromolecule-binding proteins expressed in the periplasm of strain A1 cells (Figure 2a,b). Further, UV absorption difference spectroscopy and X-ray crystallography indicated that both proteins show an affinity for alginate oligosaccharides with different M/G compositions and that these interactions are involved in the structural change of aromatic residues Tyr129, Trp270, and Trp399 in the active cleft (Table 1 and Figures 2e and 5). Although several periplasmic binding proteins have functionally and structurally been clarified (*8*, *28*), all of them are specific for small molecules. These structural and functional

Table 5: C−C Contacts between Alginate-Binding Proteins and Alginate Oligosaccharides[a]

sugar atom	bond atom	element/ domain	no. of contacts holo-AlgQ1-TE	holo-AlgQ1-DI	holo-AlgQ2-TE[b]
ΔM1					
C1	Trp270	SC2/C	6	6	6
C3	Trp270	SC2/C	2	2	2
C3	Glu396	H19/N	1	1	1
C4	Trp270	SC2/C	1	1	1
C4	Glu396	H19/N	2	2	2
C4	Trp399	L-H19:H20/N−C	1	1	1
C5	Trp270	SC2/C	5	5	5
C6	Trp270	SC2/C	6	6	6
C6	Ser273	H14/C	1	1	1
C6	Trp399	L-H19:H20/N−C	1	1	1
M2					
C2	His187	L-SC1:H9/C	−	−	1
C3	Trp270	SC2/C	2	2	1
C4	Trp270	SC2/C	2	2	2
C5	Arg20	L-SA5:SA6/N	1	1	−
C6	Tyr129	SA1/C	2	2	2
C6	Arg313	L-SC4:SA3/C−N	−	−	1
G3					
C2	Arg313	L-SC4:SA3/C−N	−		2
C3	Arg313	L-SC4:SA3/C−N	−		1
C4	Arg20	L-SA5:SA6/N	1		1
C5	Arg20	L-SA5:SA6/N	1		1
C6	Arg20	L-SA5:SA6/N	−		2
M4					
C2	Asp21	L-SA5:SA6/N	1		1
C3	Arg20	L-SA5:SA6/N	1		1
C5	Asn75	L-SA4:H3/N	1		1
C6	Trp208	L-H9:SD1/C	1		−

[a] Distance of ≤4.4 Å. [b] Results for AlgQ2 molecule A (*12*).

analyses of AlgQ1 and AlgQ2 thus provide novel information about macromolecule import.

AlgQ1 and AlgQ2 were inducibly produced in the periplasm of alginate-grown cells of strain A1. The organization of the genetic cluster for import and depolymerization of alginate in strain A1 shows that genes for the ABC importer (AlgS, AlgM1, and AlgM2) and periplasmic binding proteins (AlgQ1 and AlgQ2) constitute an operon structure (*5*), suggesting that the expression of binding proteins as well as the ABC importer is probably controlled by a promoter activated in the presence of alginate.

Although a dimeric form of AlgS is active as ATPase in vitro even after separation from the alginate ABC importer, the ATPase activity of AlgS is substantially increased in the presence of both transmembrane domains (AlgM1 and AlgM2) and periplasmic binding proteins (AlgQ1 and AlgQ2) complexed with alginate (Figure 3). This activation of ATPase is also observed in the *E. coli* maltose transport system (*29*). The purified ABC protein (MalK) for maltose import exhibits constitutive ATPase activity in the absence of maltose, but ATPase activity increases in the presence of binding protein (MalE) and its substrate. Maltose-bound MalE is better able to stimulate ATP hydrolysis than maltose-free MalE. The mechanism for association of MalE with the maltose ABC importer ($MalFGK_2$) was recently clarified (*30*). Although both maltose-bound MalE in its closed conformation and maltose-free MalE in its open conformation can interact with the importer, maltose-bound MalE initiates the transport cycle. Once MalK binds ATP, the opening of domains in MalE (release of maltose) and the periplasmic entrance produced by transmembrane domains (MalF and MalG) are induced. In the alginate import system of strain A1, activation of the ABC protein (AlgS) also requires the participation of transmembrane domains (AlgM1 and AlgM2) and alginate-bound proteins (AlgQ1 and AlgQ2), thus suggesting that information about structural change induced in binding proteins through alginate binding is transferred to the ABC protein via mediation by transmembrane domains, and the transport cycle for alginate import is similar to that for *E. coli* maltose import. To clarify the intrinsic mechanism underlying the ABC protein, we are now going to reconstitute the alginate ABC importer using AlgS, AlgM1, and AlgM2 purified independently from cells of *E. coli* containing each of these genes. We will then analyze the interaction between the ABC importer and periplasmic binding proteins.

E. coli maltose import has been well studied in the periplasmic binding protein-dependent transporter of sugar import (*8*, *10*, *30*). MalE, which has the ability to bind maltose and maltodextrin, undergoes a ligand-induced conformational change and interacts with the membrane ABC

Table 6: Changes in Backbone Torsion Angle in Hinge Connections of AlgQ1 and AlgQ2

L-SA1:SC3

	residue 132		residue 133		residue 134		residue 135		residue 136	
	ϕ (deg)	ψ (deg)	ϕ (deg)	ψ (deg)	ϕ (deg)	ψ (deg)	ϕ (deg)	ψ (deg)	ϕ (deg)	ψ (deg)
holo-AlgQ1-TE	10	9	−42	−72	39	34	28	−39	8	2
holo-AlgQ1-DI	8	17	−48	−70	37	42	18	−34	6	2
holo-AlgQ2-TE[a]	7	29	−48	29	1	17	21	−32	12	−4

L-SC4:SA3

	residue 308		residue 309		residue 310		residue 311		residue 312	
	ϕ (deg)	ψ (deg)	ϕ (deg)	ψ (deg)	ϕ (deg)	ψ (deg)	ϕ (deg)	ψ (deg)	ϕ (deg)	ψ (deg)
holo-AlgQ1-TE	−8	10	−10	13	30	−6	−10	6	4	−5
holo-AlgQ1-DI	−13	17	−16	14	29	−8	−10	6	8	−6
holo-AlgQ2-TE[a]	6	5	−7	17	6	−1	−11	15	10	6

L-H19:H20

	residue 398		residue 399		residue 400		residue 401		residue 402	
	ϕ (deg)	ψ (deg)	ϕ (deg)	ψ (deg)	ϕ (deg)	ψ (deg)	ϕ (deg)	ψ (deg)	ϕ (deg)	ψ (deg)
holo-AlgQ1-TE	−13	13	−7	−3	−8	26	6	−9	0	−4
holo-AlgQ1-DI	−11	13	−11	0	−9	32	0	−8	−5	7
holo-AlgQ2-TE[a]	−2	−1	5	0	−6	15	8	−13	6	−7

[a] Results for AlgQ2 complexed with alginate tetrasaccharide (12).

transporter. Two significant differences in substrate-binding proteins exist between alginate and maltose import, the feature of substrate and the periplasmic binding protein copy number. Alginate used in this study is a polysaccharide with more than 100 degrees of polymerization consisting of two types of highly polar sugar (M and G), while maltose and maltodextrin are composed of fewer than seven glucose residues. Two genes for periplasmic binding proteins (AlgQ1 and AlgQ2) are included in the genetic cluster for the alginate import system of strain A1. *E. coli*, in contrast, contains one type of maltose-binding protein (MalE) in the maltose operon (*10*), which is typical in the case of other *E. coli* ABC importers (*9*).

Compared to those of other periplasmic binding proteins, the binding cleft of AlgQ1 and AlgQ2 appears to extend further and longer. The surface area of the binding cleft in alginate-binding protein (AlgQ2, PDB entry 1J1N) was calculated to be 1739 Å^2 by a castP analysis (http://cast.engr.uic.edu/cast/) (*31*), while that in maltose-binding protein (MalE, PDB entry 1FRD) was 600 Å^2. MalE is shown to accommodate at most a liner tetrasaccharide in the binding cleft, although the protein can bind maltooligosaccharides composed of seven glucose residues (*32*). Computational simulation shows that at least a linear hexasaccharide can be accommodated in the active cleft of alginate-binding proteins, thus indicating that this larger space in the cleft enables AlgQ1 and AlgQ2 to bind macromolecules with high degrees of polymerization of the monosaccharide, but both alginate-binding proteins mainly recognize the first two sugar residues from the nonreducing end of alginate. The binding of two saccharides, ΔM1-M2, to S1 and S2 is the key to making the closed form. Although ΔM-M was found at the S1−S2 subsite for all three holo forms [holo-AlgQ1-TE, holo-AlgQ2-TE (*12*), and holo-AlgQ1-DI], D-guluronate may bind to S1 and S2 because similar K_d values are obtained with other alginate oligosaccharides when a G-rich tetrasaccharide mixture that should contain L-guluronate at the nonreducing end is used as a substrate for UV difference absorption spectroscopy. Since the natural form of alginate should have a saturated nonreducing end, alginate-binding proteins appear to recognize a saturated form at the S1 subsite. Further analysis of the structural features of alginate-binding proteins with native saturated and/or G-rich alginates should provide thus new insights into the mode of binding.

Distinct from other bacteria, cells of strain A1 produce two types of periplasmic alginate-binding proteins (AlgQ1 and AlgQ2) in the periplasm that are similar in primary structure. Yet what is the purpose of this? In this work, we thoroughly analyzed the structure and function of AlgQ1 and AlgQ2 but failed to find significant differences between them except for an altered rotation angle between N and C domains. AlgQ1 and AlgQ2 share the following structural and functional features: an overall structure consisting of N and C domains with a deep cleft, conformational change of two domains in the binding or release of alginate, dissociation constant (K_d) toward alginate and its oligosaccharides, substrate specificity, and optimal binding pH. We thus concluded that AlgQ1 and AlgQ2 likely arose due to gene duplication in cells of strain A1.

Through comparative genomics, our conclusion is supported by the organization of a certain genetic cluster in *Agrobacterium tumefaciens* (*33*). The genetic cluster homologous to that for alginate import and degradation of strain A1 is included in the *Agrobacterium* genome, and consists of five genes encoding hypothetical proteins, Atu3021, Atu3022, Atu3023, Atu3024, and Atu3025, showing significant homology with AlgS (60% identical), AlgM1 (62%), AlgM2 (67%), AlgQ1 (56%), and A1-IV (55%), respectively. Due to the high degree of similarity, hypothetical proteins are assigned to those responsible for sugar import and degradation. The *Agrobacterium* genetic cluster contains a single gene encoding an alginate-binding protein homologue. We therefore postulate that the genetic cluster for alginate import and degradation is transferred horizontally from that of the *Agrobacterium*-like bacteria to strain A1, and two copies of the alginate-binding protein are generated through gene duplication in strain A1.

ACKNOWLEDGMENT

X-ray diffraction experiments were conducted at beamline BL44XU of SPring-8 (Proposal C01A44XU-7136-N).

REFERENCES

1. Gacesa, P. (1988) Alginates, *Carbohydr. Polym. 8*, 161−182.
2. Wong, T. Y., Preston, L. A., and Schiller, N. L. (2000) Alginate lyase: Review of major sources and enzyme characteristics, structure−function analysis, biological roles, and applications, *Annu. Rev. Microbiol. 54*, 289−340.
3. Hisano, T., Yonemoto, Y., Yamashita, T., Fukuda, Y., Kimura, A., and Murata, K. (1995) Direct uptake of alginate molecules through a pit on the bacterial cell surface: A novel mechanism for the uptake of macromolecules, *J. Ferment. Bioeng. 79*, 538−544.
4. Hisano, T., Kimura, N., Hashimoto, W., and Murata, K. (1996) Pit structure on bacterial cell surface, *Biochem. Biophys. Res. Commun. 220*, 979−982.
5. Momma, K., Okamoto, M., Mishima, Y., Mori, S., Hashimoto, W., and Murata, K. (2000) A novel bacterial ATP-binding cassette (ABC) transporter system that allows uptake of macromolecules, *J. Bacteriol. 182*, 3998−4004.
6. Yoon, H.-J., Hashimoto, W., Miyake, O., Okamoto, M., Mikami, B., and Murata, K. (2000) Overexpression in *Escherichia coli*, purification, and characterization of *Sphingomonas* sp. A1 alginate lyases, *Protein Expression Purif. 19*, 84−90.
7. Hashimoto, W., Miyake, O., Momma, K., Kawai, S., and Murata, K. (2000) Molecular identification of oligoalginate lyase of *Sphingomonas* sp. strain A1 as one of the enzymes required for complete depolymerization of alginate, *J. Bacteriol. 182*, 4572−4577.
8. Davidson, A. L., and Chen, J. (2004) ATP-binding cassette transporters in bacteria, *Annu. Rev. Biochem. 73*, 241−268.
9. Linton, K. J., and Higgins, C. F. (1998) The *Escherichia coli* ATP-binding cassette (ABC) proteins, *Mol. Microbiol. 28*, 5−13.
10. Boos, W., and Shuman, H. (1998) Maltose/maltodextrin system of *Escherichia coli*: Transport, metabolism, and regulation, *Microbiol. Mol. Biol. Rev. 62*, 204−229.
11. Momma, K., Mikami, B., Mishima, Y., Hashimoto, W., and Murata, K. (2002) Crystal structure of AlgQ2, a macromolecule (alginate)-binding protein of *Sphingomonas* sp. A1 at 2.0 Å resolution, *J. Mol. Biol. 316*, 1061−1069.
12. Mishima, Y., Momma, K., Hashimoto, W., Mikami, B., and Murata, K. (2003) Crystal structure of AlgQ2, a macromolecule (alginate)-binding protein of *Sphingomonas* sp. A1, complexed with an alginate tetrasaccharide at 1.6-Å resolution, *J. Biol. Chem. 278*, 6552−6559.
13. Sambrook, J., Fritsch, E. F., and Maniatis, T. (1989) *Molecular cloning: A laboratory manual*, 2nd ed., Cold Spring Harbor Laboratory Press, Plainview, NY.
14. Mizushima, S., and Yamada, H. (1975) Isolation and characterization of two outer membrane preparations from *Escherichia coli*, *Biochim. Biophys. Acta 375*, 44−53.
15. Sanger, F., Nicklen, S., and Coulson, A. R. (1977) DNA sequencing with chain-terminating inhibitors, *Proc. Natl. Acad. Sci. U.S.A. 74*, 5463−5467.

16. Bradford, M. M. (1976) A rapid and sensitive method for the quantification of microgram quantities of protein utilizing the principle of protein-dye binding, *Anal. Biochem. 72*, 248−254.
17. Laemmli, U. K. (1970) Cleavage of structural proteins during the assembly of the head of bacteriophage T4, *Nature 227*, 680−685.
18. Hashimoto, W., Suzuki, H., Yamamoto, K., and Kumagai, H. (1995) Effect of site-directed mutations on processing and activity of γ-glutamyltranspeptidase of *Escherichia coli* K-12, *J. Biochem. 118*, 75−80.
19. Hashimoto, W., Okamoto, M., Hisano, T., Momma, K., and Murata, K. (1998) *Sphingomonas* sp. A1 lyase active on both poly-β-D-mannuronate and heteropolymeric regions in alginate, *J. Ferment. Bioeng. 86*, 236−238.
20. Pflugrath, J. W. (1999) The finer things in X-ray diffraction data collection, *Acta Crystallogr. D55*, 1718−1725.
21. Collaborative Computational Project No. 4 (1994) The CCP4 suite: Programs for protein crystallography, *Acta Crystallogr. D50*, 760−763.
22. Brünger, A. T., Adams, P. D., Clore, G. M., DeLano, W. L., Gros, P., Grosse-Kunstleve, R. W., Jiang, J. S., Kuszewski, J., Nilges, M., Pannu, N. S., Read, R. J., Rice, L. M., Simonson, T., and Warren, G. L. (1998) Crystallography and NMR system: A new software suite for macromolecular structure determination, *Acta Crystallogr. D54*, 905−921.
23. Berman, H. M., Westbrook, J., Feng, Z., Gilliland, G., Bhat, T. N., Weissig, H., Shindyalov, I. N., and Bourne, P. E. (2000) The protein data bank, *Nucleic Acids Res. 28*, 235−242.
24. Laskowski, R. A., MacArthur, M. W., Moss, D. S., and Thornton, J. M. (1993) PROCHECK: A program to check the stereochemical quality of protein structures, *J. Appl. Crystallogr. 26*, 283−291.
25. Kraulis, P. J. (1991) MOLSCRIPT: A program to produce both detailed and schematic plots of protein structure, *J. Appl. Crystallogr. 24*, 946−950.
26. Merrit, E. A., and Murphy, M. E. P. (1994) RASTER3D Version 2.0: A program for photorealistic molecular graphics, *Acta Crystallogr. D50*, 869−873.
27. Ramachandran, G. N., and Sasisekharan, V. (1968) Conformations of polypeptides and proteins, *Adv. Protein Chem. 23*, 283−437.
28. Quiocho, F. A., and Ledvina, P. S. (1996) Atomic structure and specificity of bacterial periplasmic receptors for active transport and chemotaxis: Variation of common themes, *Mol. Microbiol. 20*, 17−25.
29. Davidson, A. L., Shuman, H. A., and Nikaido, H. (1992) Mechanism of maltose transport in *Escherichia coli*: Transmembrane signaling by periplasmic binding proteins, *Proc. Natl. Acad. Sci. U.S.A. 89*, 2360−2364.
30. Austermuhle, M. I., Hall, J. A., Klug, C. S., and Davidson, A. L. (2004) Maltose-binding protein is open in the catalytic transition state for ATP hydrolysis during maltose transport, *J. Biol. Chem. 279*, 28243−28250.
31. Liang, J., Edelsbrunner, H., and Woodward, C. (1998) Anatomy of protein pockets and cavities: Measurement of binding site geometry and implications for ligand design, *Protein Sci. 7*, 1884−1897.
32. Quiocho, F. A., Spurlino, J. C., and Rodseth, L. E. (1997) Extensive features of tight oligosaccharide binding revealed in high-resolution structures of the maltodextrin transport/chemosensory receptor, *Structure 5*, 997−1015.
33. Goodner, B., Hinkle, G., Gattung, S., Miller, N., Blanchard, M., Qurollo, B., Goldman, B. S., Cao, Y., Askenazi, M., Halling, C., Mullin, L., Houmiel, K., Gordon, J., Vaudin, M., Iartchouk, O., Epp, A., Liu, F., Wollam, C., Allinger, M., Doughty, D., Scott, C., Lappas, C., Markelz, B., Flanagan, C., Crowell, C., Gurson, J., Lomo, C., Sear, C., Strub, G., Cielo, C., and Slater, S. (2001) Genome sequence of the plant pathogen and biotechnology agent *Agrobacterium tumefaciens* C58, *Science 294*, 2323−2328.

BI047781R